HHS Public Access

Author manuscript

Gastroenterology. Author manuscript; available in PMC 2016 July 01.

Published in final edited form as:

Gastroenterology. 2015 July ; 149(1): 56–66.e5. doi:10.1053/j.gastro.2015.04.003.

Loss of Interstitial Cells of Cajal and Patterns of Gastric Dysrhythmia in Patients with Chronic Unexplained Nausea and Vomiting

Timothy R. Angeli[1], **Leo K. Cheng**[1,2], **Peng Du**[1], **Tim Hsu-Han Wang**[3], **Cheryl E. Bernard**[4], **Maria-Giuliana Vannucchi**[5], **Maria Simonetta Faussone-Pellegrini**[5], **Christopher Lahr**[6], **Ryash Vather**[3], **John A. Windsor**[3], **Gianrico Farrugia**[4], **Thomas L. Abell**[7], and **Gregory O'Grady**[1,3,*]

[1]Auckland Bioengineering Institute, University of Auckland, Auckland, New Zealand [2]Department of Surgery, Vanderbilt University, Nashville, Tennessee, USA [3]Department of Surgery, University of Auckland, Auckland, New Zealand [4]Division of Gastroenterology and Hepatology, and Enteric Neurosciences Program, Mayo Clinic, Rochester, Minnesota, USA [5]Histology and Embryology Research Unit, Department of Experimental and Clinical Medicine, University of Florence, Italy [6]Department of Surgery, Mississippi Medical Center, Jackson, Mississippi, USA [7]Department of Gastroenterology, University of Louisville, Louisville, Kentucky, USA

Abstract

Background & Aims—Chronic unexplained nausea and vomiting (CUNV) is a debilitating disease of unknown cause. Symptoms of CUNV substantially overlap with those of gastroparesis, so the diseases therefore may share pathophysiologic features. We investigated this hypothesis by quantifying densities of interstitial cells of Cajal (ICCs) and mapping slow wave abnormalities in patients with CUNV vs controls.

Methods—Clinical data and gastric biopsy specimens were collected from 9 consecutive patients with at least 6 months of continuous symptoms of CUNV, but normal gastric emptying, treated at the University of Mississippi Medical Center, and from 9 controls (individuals undergoing bariatric surgery but free of gastrointestinal disease or diabetes). ICCs were counted and ultrastructural analyses were performed on tissue samples. Slow-wave propagation profiles were defined by high-resolution electrical mapping (256 electrodes; 36 cm^2). Results from patients with CUNV were compared to those of controls as well as patients with gastroparesis who were previously studied by identical methods.

Results—Patients with CUNV had fewer ICCs than controls (mean 3.5 vs 5.6 bodies/field; $P<.05$), with mild ultrastructural abnormalities in the remaining ICCs. Slow-wave dysrhythmias were

*Corresponding Author: Dr. Gregory O'Grady, Dept. of Surgery, University of Auckland, Private Bag 92019, Auckland, New Zealand, +64 (21) 422 2989 (phone); +64 9 367 7157 (fax), greg.ogrady@auckland.ac.nz.

Author contributions: Study concept and design: GOG, TRA, LKC, TLA, GF. Data collection: TRA, GOG, CL, PD, JAW, RV, LKC, TLA. Data analysis and interpretation: TRA, GOG, TW, CEB, GF, TLA, LKC, MGV, MSFP. Drafting of manuscript: TRA, GOG. Critical review of manuscript: LKC, GF, TLA, JAW, RV, PD, TW, CEB, CL, MGV, MSFP.

Competing interests: No authors have any financial or other competing interests in relation to the material presented in this paper.

identified in all 9 subjects with CUNV vs only 1/9 controls. Dysrhythmias included abnormalities of initiation (stable ectopic pacemakers, unstable focal activities) and conduction (retrograde propagation, wave front collisions, conduction blocks, and re-entry), operating across bradygastric, normal (range 2.4−3.7 cycles/min), and tachygastric frequencies; dysrhythmias showed velocity anisotropy (mean 3.3 mm/s longitudinal vs 7.6 mm/s circumferential, $P<.01$). ICCs were less depleted in patients with CUNV than those with gastroparesis (mean 3.5 vs 2.3 bodies/field; $P<.05$), but slow-wave dysrhythmias were similar between groups.

Conclusions—This study defined cellular and bioelectrical abnormalities in patients with CUNV, including the identification of slow-wave re-entry. Pathophysiologic features of CUNV were observed to be similar to those of gastroparesis, indicating that they could be spectra of the same disorder. These findings offer new insights into the pathogenesis of CUNV and may help to inform future treatments.

Keywords

slow wave; high-resolution mapping; gastroparesis; ICC

INTRODUCTION

Chronic unexplained nausea and vomiting (CUNV) is a relatively uncommon but debilitating disease. The cause is currently unknown, with patients exhibiting chronic gastric symptoms while demonstrating normal gastric emptying and lacking obstruction or obvious structural abnormality.[1,2]

Pasricha *et al.* recently comprehensively reported the clinical features of CUNV.[2] It was found that the features of this disorder overlap substantially with gastroparesis, being almost identical in terms of demographics, symptoms, disease duration, health care utilization, and quality of life. Similar observations have also been reported elsewhere.[3,4] Pasricha *et al.* concluded that CUNV is poorly defined and not adequately categorized by Rome III criteria, and that further research was needed to determine whether CUNV is part of a spectrum of the same syndrome as gastroparesis, or represents a distinct disorder(s).[2]

There has been substantial recent progress in understanding the pathogenic mechanisms of gastroparesis,[5,6] and among several contributing factors, there is an increasing focus on the role played by interstitial cells of Cajal (ICC). ICC depletion is now recognized as the predominant cellular abnormality in gastroparesis.[7–9] By contrast, few studies to date have investigated the mechanisms underlying CUNV,[10] and a role for ICC has not been adequately evaluated.

ICC generate and propagate slow waves, which coordinate phasic gastric contractions, and ICC loss in gastroparesis is known to be associated with dysrhythmic slow wave activity.[9,11] In particular, a recent study, using new techniques of high-resolution (HR), multi-electrode mapping,[12] demonstrated a range of abnormal slow wave initiation and conduction patterns in most patients with gastroparesis, which were not observed in controls.[9] Gastric dysrhythmias are associated with nausea and vomiting, potentially causing these symptoms,

and could therefore be contributing to the pathophysiology and symptomatology of both CUNV and gastroparesis.[13,14]

In this study, we hypothesized that ICC depletion and spatially-complex slow wave dysrhythmias occur in CUNV, as has been found in gastroparesis. This hypothesis was tested by performing ICC density and ultrastructural analyses, in combination with *in-vivo* HR gastric mapping in a cohort of CUNV patients, with comparison to new controls and gastroparetic patients previously investigated using identical methods.

METHODS

Ethical approval was granted by the New Zealand Regional Ethics Committee, and by the Institutional Review Boards at The University of Mississippi and Mayo Clinic. All patients provided informed consent.

Patients

CUNV Cohort: Consecutive patients with at least six months of continuous symptoms of CUNV who were undergoing implantation of gastric electrical stimulation devices at the University of Mississippi Medical Center were invited to participate. All patients had a history, drug history, physical examination, upper endoscopy, and appropriate radiological and laboratory investigations to exclude other causes of symptoms. Patients with cyclic vomiting syndrome were excluded.[15] Patients were also excluded if they had gastroparesis, as diagnosed by scintigraphy testing according to a standardized test meal[16] and consensus recommendations (>60% retention at 2 hours and / or >10% gastric retention at 4 hours),[2,17] or malignancy, primary eating disorders, or pregnancy. Hyperglycemia can induce dysrhythmias,[18] and blood glucose was kept within the normal range during the perioperative period.

Demographic data, comorbidities, medical histories, and body mass index were recorded. Total symptom scores were calculated by scoring five symptoms (pain, bloating / distension, nausea, vomiting, and early satiety) on a five-point scale (0, absent; 4, severe).[9]

ICC Controls were age-matched patients undergoing bariatric surgery, who were free of gastrointestinal diseases or diabetes. Obesity does not affect ICC numbers,[7] but age matching was performed because ICC decrease by approximately 13% per decade.[19]

HR mapping controls were patients undergoing elective upper-abdominal surgery. Patients were excluded if they had previous gastric surgery, known gastric pathology, or a condition in which dysrhythmic gastric activity has been described, including gastroparesis, gastric tumors, pregnancy, anorexia nervosa, functional dyspepsia, atrophic gastritis, or hypo- or hyperthyroidism.[13,20] Control patients were not taking gastric prokinetics or medications affecting gastric electrical activity.

A historical cohort of gastroparetic patients was utilized for further comparison.[9] These patients underwent HR gastric mapping and ICC density analysis using identical methods, at the same institutions.

ICC Density and Ultrastructural Analysis

Full-thickness gastric biopsy specimens were collected from the anterior stomach, midway between the curvatures and approximately 9 cm proximal to the pylorus. This site is the same as that chosen by the Gastroparesis Clinical Research Consortium (GpCRC) in their studies of cellular defects in gastroparesis.[7,8] ICC cell bodies in the circular muscle layer were identified using a Kit antibody (mouse 1:400; Lab Vision MS-482-P; Thermo Fisher Scientific, Waltham, MA) and a 4-,6-diamidino-2-phenylindole (DAPI) nucleus counterstain, where co-localization of a DAPI-positive nucleus within a Kit-positive ICC signified an ICC cell body. Using the methods described by Grover *et al*[7,21] ICC density was calculated by quantifying the number of cell bodies per field across 20 high-powered fields per specimen. Electron microscopy studies of ICC were also performed on CUNV and control tissues using previously described methodology.[8]

High-Resolution Electrical Mapping

HR mapping was performed using established and validated extracellular methods.[9,22,23] Flexible printed circuit board (PCB) electrode arrays were used (96–256 electrodes; 4–5.2 mm interelectrode spacing; Figure 1A).[24] All recordings were performed intraoperatively after general anesthesia and laparotomy (Table 1). These anesthetic conditions are not known to affect slow waves,[22,25] except for the use of opiates, which may be associated with myoelectrical abnormalities.[26]

Mapping was undertaken before organ handling or stimulator placement. The PCBs were laid on the anterior serosa with reference to gastric landmarks.[22] Warm saline-soaked gauze was overlain, and the cables were allowed to move freely with respiration. Patients were mapped for up to 15 minutes, over 1–3 gastric regions. Reference electrodes were placed on the shoulders and unipolar signals were acquired at 512 Hz using an ActiveTwo System (Biosemi, The Netherlands) modified for passive recordings.

Signal Processing, Analysis, and Interpretation

HR mapping data was analyzed in the Gastrointestinal Electrical Mapping Suite (GEMS), v. 1.5.[27] Recordings were down-sampled (30 Hz) and filtered with moving-median and Savitzky-Golay filters.[28] Slow wave activation times were identified using the FEVT algorithm,[29] and were clustered into cycles using the REGROUPS algorithm,[30] with manual correction. Activation maps were calculated (e.g., Figure 1),[30] and sites of conduction block were identified. Slow wave propagation animations were generated.[27]

Frequency was calculated by averaging the cycle-to-cycle intervals between activation times. The normal human gastric slow wave frequency was defined as 2.4 – 3.7 cycles/min based on electrogastrography literature.[31] Velocity was calculated using a finite difference method with Gaussian-smoothing filter, and visualized using directional arrows on a color-gradient speed map.[32] In addition, velocity was secondarily averaged across regions of circumferential and longitudinal propagation, to investigate conduction anisotropy.[33] Amplitudes were calculated by applying a peak-to-trough detection algorithm.[28]

All data were screened for dysrhythmias by isochronal mapping and animation.[27] Dysrhythmias were identified, defined, and quantified by frequency, rhythm (stable vs unstable), and spatial pattern (abnormalities of initiation and/or conduction), using established methods.[9,34,35] Data were expressed as a mean ± SD or SEM, or median and range. Student's *t* test was used for the statistical analyses, unless otherwise noted, with a significance threshold of $P < 0.05$.

RESULTS

Study Populations

The CUNV cohort consisted of 9 consecutive patients (4 diabetic), with median 4-hour gastric retention of 4% (range 2 – 9%) and median total symptom score of 16/20 (range 9.5–20). The mean time from gastric emptying test to surgery was 2.1 ± 2.3 months. The HR mapping controls also consisted of 9 patients, of comparable age to the CUNV cohort (P=0.14). Table 1 compares the CUNV and HR mapping control populations, with individual patient data provided in Supplementary Tables 1 and 2. The ICC control cohort was appropriately age-matched to the CUNV cohort (paired mean difference 0.3 years; P=0.8).

ICC Density and Ultrastructural Analysis

Tissue specimens were obtained from 7/9 CUNV patients. Figure 2 shows representative images comparing ICC density and ultrastructural features between CUNV patients and controls. Overall, average ICC density was reduced in CUNV patients compared to controls (mean 3.5 ± 0.3 SEM vs 5.6 ± 0.5 cell bodies/field; P<0.05; Figure 3). There was no difference between ICC densities from CUNV patients with diabetes versus without (P=0.9). Individual ICC densities for the CUNV patients are reported in Supplementary Table 1 (range: 2.8 – 4.7 cell bodies/field).

The results for ICC density in CUNV patients were then compared with the historical gastroparetic cohort (mean 2.3 ± 0.3 SEM bodies/field), collected and analyzed using identical protocols.[9] A one-way ANOVA between the CUNV, gastroparesis, and combined-control cohorts showed that ICC density differed significantly across the three groups (P<0.05). A Newman-Keuls post-hoc comparison between the three groups indicated that the combined controls had higher ICC density than the CUNV (P<0.05; mean difference: 2.0 bodies/field) and gastroparesis (P<0.05; mean difference: 3.2 bodies/field) cohorts. In addition, ICC density was higher in the CUNV than gastroparesis cohort (P<0.05; mean difference: 1.2 bodies/field; Figure 3).

Ultrastructural analyses revealed abnormalities in the ICC of 5/7 sampled CUNV patients compared to matched controls (Figure 2C,D). These abnormalities were less severe than those previously reported in gastroparesis,[8] primarily consisting of thickened basal lamina, particularly near nerve endings, smooth muscle cells, and nerve fibers, as well as scattered cytoplasmic anomalies including lamellar bodies, dilated reticulum, vacuoles, and myelin bodies (Figure 2C).

High-Resolution Electrical Mapping

Controls—A total of 11 recordings were performed on the 9 controls at the mid-to-lower gastric corpus and antrum (Figure 1), with a mean recording duration of 10 ± 3 SD min/patient. The mean slow wave frequency across the control cohort was 2.7 ± 0.1 SEM cycles/min. In 8/9 patients, entirely normal gastric activation patterns were observed; slow wave activity propagated exclusively in the antegrade direction with wavefronts oriented orthogonal to the curvatures (Figure 1). In these 8 controls, all activity was consistent with the established single pacemaker system of the normal human stomach (mean corpus velocity 3.0 ± 0.3 SEM mm/s).[22]

In one control (ID #4 in Supplementary Table 2), dysrhythmic slow wave activity was observed. At the time of mapping this patient, it was noted that the stomach was significantly distended with air following pre-oxygenation and intubation. This dysrhythmia occurred as a stable ectopic pacemaker in the mid-corpus, was present at the onset of mapping, and persistent for 330 seconds before becoming entrained by normal antegrade activity (Supplementary Figure 1).

CUNV Patients—A total of 18 recordings were performed on the corpus and antrum of the 9 CUNV patients, with a mean duration of 11 ± 5 SD min/patient, which was comparable to the control recordings ($P = 0.7$). Dysrhythmic slow wave activity was observed in all 9/9 patients, and the observed dysrhythmias were classified as abnormalities of initiation (8/18 recordings; 6/9 patients) or abnormalities of conduction (11/18 recordings; 8/9 patients). Abnormalities of initiation and conduction coexisted in 5/9 patients. These dysrhythmic patterns were further classified according to the schema summarized in Figure 4.

Across all CUNV patients, the mean frequency during dysrhythmic slow wave activity was 3.3 ± 0.3 SEM cycles/min (range 2.0 – 5.1 cycles/min), which was similar to that of controls ($P > 0.05$). Dysrhythmias occurred at normal frequency in 5/9 patients, bradygastric frequency (<2.4 cycles/min) in 2/9 patients, and tachygastric frequency (>3.7 cycles/min) in 2/9 patients.

Slow wave activity propagated at a mean longitudinal velocity of 3.3 ± 0.6 SEM mm/s in the dysrhythmic CUNV cohort, which was similar to that in controls ($P = 0.7$). Circumferential propagation was also routinely observed during dysrhythmia and exhibited a highly anisotropic velocity profile, whereby propagation occurred more rapidly in the circumferential direction (mean 7.6 ± 1.5 SEM mm/s) than the longitudinal direction ($P < 0.01$). During longitudinal propagation, the extracellular slow wave amplitudes were comparable between CUNV patients and controls (mean 0.30 ± 0.08 SEM vs 0.33 ± 0.05 mV; $P = 0.7$).

Abnormalities of Slow Wave Initiation—Abnormal initiation of slow wave activity was identified in 8/18 recordings from 6/9 patients (Figure 5 and Supplementary Figure 2), whereby slow wave activity was initiated from a location other than the normal gastric pacemaker region (greater curvature, mid-to-upper corpus[22]). These abnormalities of initiation were further classified as either stable (occurring consistently in the same location over time) or unstable (transient focal activities occurring in variable locations). Stable

ectopic initiation (ectopic pacemaking; e.g., Supplementary Figure 2) was the most prevalent abnormality of initiation, observed in 4 patients, and occurring for a mean captured duration of 109 ± 42 SD s, although all instances were either present at the beginning, or persistent through the end, of the recording period. Unstable ectopic focal activities were observed in 2 patients, and lasted for only 18 s (1 cycle) and 50 s (2 cycles; Figure 5C, D), respectively.

Abnormal slow-wave initiation occurred at mean frequency of 3.1 ± 0.5 SEM cycles/min (range 2.0 – 5.1 cycles/min), with individual ectopic events occurring at bradygastric (1 stable; 1 unstable), normal (3 stable), and tachygastric (1 unstable) frequencies. One patient (Figure 5; ID #2, Supplementary Table 1) displayed unstable focal activity for two cycles at bradygastric frequency (mean 2.0 ± 0.1 SD cycles/min; Figure 5C, D), which was then entrained by a new stable ectopic pacemaker occurring at a normal frequency (mean 3.2 ± 0.2 SD cycles/min; Figure 5E, F) that continued to the end of the recording period.

Ectopic slow wave initiation was always associated with disorganized slow wave propagation. These patterns were characterized as secondary abnormalities of conduction and are described in the following section.

A third abnormality of slow wave initiation was observed in three recordings from a single patient (ID #1, Supplementary Table 1), whereby a complete lack of slow wave initiation and activity occurred across the entire mapped field of all three consecutive recordings. The electrode signals from these recordings exhibited stable baseline activity with low noise, and cardiac signal complexes were clearly distinguishable under modified filtering parameters (Supplementary Figure 3), indicating that the electrodes were functioning and that satisfactory contact with the serosal surface had been achieved.

Abnormalities of Slow Wave Conduction—Abnormalities of slow wave conduction occurred in 11/18 recordings in 8/9 patients and included conduction blocks, re-entrant activity, retrograde propagation, and colliding wavefronts.

Conduction blocks occurred in 4/9 patients, whereby slow wave activation terminated abnormally. In one case (Figure 5), a complete conduction block manifested between uncoupled slow wave activation propagating in opposite directions, where the block extended the entire width of the mapped area. In the other three cases of observed conduction blocks, the blocks were incomplete, inducing a wavelet that subsequently excited the tissue region distal to the block (e.g., Supplementary Figure 4).

Re-entrant slow wave activity occurred in a single patient, whereby wavefronts propagated in a complete loop around a line of unidirectional block, continuously re-activating the same tissue circuit over successive cycles (Figure 6). Wavefronts emanated outward from the site of re-entry (mean frequency 3.3 ± 0.2 SD cycles/min), establishing propagation in all directions and resulting in wavefront collisions with antegrade-propagating wavefronts. In addition, there was one further case of conduction block with looping propagation pattern that was incompletely captured by the mapped field, and was therefore classified as being of

indeterminate origin. This dysrhythmia operated at a tachygastric frequency (mean 4.3 ± 0.3 SD cycles/min).

In general, disorganized slow wave propagation occurred secondary to all of the previously described abnormalities of initiation and conduction, and was quantified as retrograde propagation and wavefront collisions. Retrograde propagation occurred in 10/18 recordings across 8/9 patients, originating from ectopic pacemakers (5 recordings), sites of re-entry (1 recording), and unidentified sites outside the mapped field (4 recordings). Retrograde propagation occurred at a mean velocity of 3.3 ± 0.7 SEM mm/s, which was comparable to that of antegrade propagation in controls (mean 3.0 ± 0.3 SEM mm/s; $P = 0.7$) and CUNV (mean 3.3 ± 0.6 SEM mm/s; $P = 0.9$), demonstrating directional velocity isotropy in the longitudinal axis of the human stomach.

Wavefront collisions occurred in 7/18 recordings across 5/9 patients, where a retrograde or circumferentially-propagating wavefront collided with opposing propagation (e.g., Figures 5 and 6, and Supplementary Figure 2). Wavefront collisions were associated with wavefronts originating from ectopic pacemakers (4 recordings; e.g., Figure 5 and Supplementary Figure 2), unidentified sources located outside of the mapped field (2 recordings), and re-entry (1 recording; Figure 6).

Normal Slow Wave Propagation—Although all CUNV patients exhibited some form of dysrhythmic activity during at least one of their recording periods, a subset of 4/18 recordings from 3/9 patients displayed a normal slow wave propagation pattern for the entire recorded duration. This normal propagation occurred at a mean frequency of 2.8 ± 0.2 SEM cycles/min (range 2.4 – 3.2 cycles/min) and propagated at a mean longitudinal velocity of 2.8 ± 0.6 SEM mm/s, both of which were similar to that of controls ($P = 0.8$ and 0.6, respectively).

DISCUSSION

CUNV is accompanied by considerable morbidity, but has remained a poorly characterized disorder of unknown etiology. This study quantified ICC numbers and ultrastructural features, in combination with modern slow wave mapping techniques,[12] to investigate pathogenic mechanisms contributing to CUNV. It was found that CUNV patients had ICC depletion and abnormal slow wave initiation and conduction, compared to controls. Further comparison to a historic cohort of gastroparetic patients[9] revealed that ICC depletion and ultrastructural abnormalities were less severe in CUNV than in gastroparesis, but abnormalities of slow wave initiation and conduction were similar. The cellular and electrophysiological abnormalities observed in this study offer plausible contributing mechanisms to the pathophysiology of CUNV.

This study was partly motivated by a recent report by Pasricha *et al.*, which provided the first comprehensive account of the demographic and clinical features of CUNV.[2] CUNV was shown to be clinically indistinguishable from gastroparesis over a one-year follow-up period, which is consistent with other literature.[3,4] Pasricha *et al.* concluded that further research was needed to conclusively determine whether CUNV is part of a spectrum of the

same syndrome as gastroparesis, or represents a distinct disorder(s).[2] Both conclusions may hold truth as CUNV is likely heterogeneous. However, our study does support the idea that CUNV may, at least in part, be encompassed within the same disease spectrum as gastroparesis, by demonstrating that these disorders share common cellular and bioelectrical pathophysiologies.[7,9] Of note, the ICC depletion and ultrastructural abnormalities in the CUNV cohort were less marked than in previous gastroparesis cohorts analyzed by equivalent methods,[8,9] and the actual ICC densities are consistent with a previous observation that depletion of less than 3 ICC bodies per field may represent a threshold below which failure of gastric emptying becomes more likely.[19] Gastric distension has been ruled out as a confounding factor in ICC counts using comparative smooth muscle nuclei counts.[9]

We focused on ICC because they are the predominant cellular abnormality in gastroparesis,[7] and because ICC densities correlate with gastric emptying, unlike other markers.[21] However, ICC, neuronal, and smooth muscle pathologies often co-exist, perhaps due to cellular interdependence, and it is not always clear which changes hold primacy.[36] Other histologic abnormalities described in gastroparesis include an immune cell infiltrate typified by CD45 and CD68 immunoreactivity, decreased nerve fibres,[7] and ultrastructural degradation of remaining ICC.[8] These factors were not a focus of the present study, but would be of interest in future studies of CUNV.

The HR mapping outcomes reported in this study corroborate and expand the known range of dysrhythmic human slow wave patterns. These patterns have been accurately assessed in only one previous study in gastroparetic patients,[9] of which the results of the present study are consistent. CUNV and gastroparesis both showed heterogeneous patterns of abnormal initiation and conduction, including stable and unstable ectopic pacemaking, conduction blocks, and secondary propagation abnormalities of retrograde propagation and colliding wavefronts. It was also shown that human gastric dysrhythmias routinely occurred within a frequency range considered normal, while normal activity could occur at frequencies sometimes considered abnormal, challenging ‘normal’ frequency conceptions.[31] These results validate and reinforce that spatial mapping enables a substantially more accurate method of dysrhythmia detection than classical electrogastrography, which mainly focused on frequency[31] and therefore likely underestimated the occurrence of slow wave abnormalities. The results from the present study also facilitate an updated classification schema for human gastric dysrhythmias, focused on spatial pattern.[9] Furthermore, the finding that a subset of 4/18 recordings exhibited normal activity demonstrated that multiple recordings, or at least sustained recordings of greater than about five minutes, may be necessary to consistently detect dysrhythmic activity.

This study described re-entrant slow wave activity in the human gut. Originally described by Lammers *et al.* in 2008 in a canine model,[37] and subsequently in several other *invitro* and *in-vivo* animal models,[34,35,38] re-entry is now a focus of considerable recent interest as a mechanism of sustained gastrointestinal dysrhythmias.[39] Based on our findings, re-entry is a relatively uncommon dysrhythmia in the human stomach, likely because there is a narrow excitable gap, or window, in which an aberrant stimulus can successfully invoke a re-entry, based on the relative timing of the leading depolarizing edge and refractory tail.[34,35,39] Re-

entry is also an important finding because it is a potentially treatable form of dysrhythmia, for example, by gastric pacing guided by mapping,[40] as is routinely achieved in cardiology.

The fact that CUNV patients had normal gastric emptying despite pronounced dysrhythmia is consistent with previous literature, which has shown an overall positive predictive value of EGG abnormalities for abnormal gastric emptying of only ~65%.[31] Significantly, gastric emptying shows no correlation with nausea and vomiting, while dysrhythmia shows consistent correlations with these symptoms across multiple disease states.[2,13] It is therefore evident that the stomach has compensatory mechanisms that may preserve emptying despite dysrhythmias, including the rapid circumferential conduction evident in this study, which may aid in restoring propulsive ring contractions distal to dysrhythmic events.[9,33] Together with dysrhythmias, other ICC abnormalities occurring in gastroparesis could cumulatively be contributing to delayed emptying. For example, residual ICC in gastroparesis show marked cellular damage, and may generate a reduced volume of current to excite smooth muscle.[8,9,13] ICC roles in modulating resting membrane gradients, neurotransmission, and mechanotransduction could also be significant, but more research is needed. The presence of a thickened basal lamina at the contact between ICC and nerve endings in CUNV patients is suggestive of impairment in the crosstalk, which in turn could influence the ICC rhythmic activity. Further studies are now required to investigate mechanisms by which ICC damage causes dysrhythmia, and how dysrhythmia causes nausea and vomiting, with current evidence suggesting such causal associations are plausible.[13]

One control subject exhibited dysrhythmic slow wave activity, characterized by tachygastric ectopic pacemaking in the mid-corpus. This represents the only instance of slow wave dysrhythmia in 21 normal controls mapped to date (9 in this study, 12 in a previous study[22]), and may have occurred due to excessive gastric distension in this patient following anesthetic induction and intubation. A similar type of dysrhythmic initiation has previously been described with antral balloon distension in healthy humans.[41] It may prove necessary to exclude subjects showing gastric distension in future studies. It is also possible that normal subjects have episodes of self-correcting dysrhythmia. The research implication of this dysrhythmic finding in a control patient was that it provided an opportunity to quantify circumferential conduction parameters in the healthy human stomach. The observed conduction profile in this patient exhibited velocity anisotropy similar to that observed in the ICC-depleted CUNV cohort, and also previously observed in animals and ICC-depleted gastroparetic humans.[9,33]

The main limitation of this study was the relatively small sample size. However, the current limited cohort is unique because intraoperative access is rare in CUNV patients, and the operative gastric stimulator implantation that allowed surgical access for this study is usually only offered for gastroparesis. Furthermore, this study also required the recruitment of intra-operative mapping controls. Because the mapping in this study required surgical access, it was performed in the anesthetized state; it would be desirable to investigate these slow wave patterns in awake, fed, and fasted patients, when future technological advances allow. While we chose the definition ‘CUNV’ following Pasricha *et al.*,[2] such nomenclature is not standardized. Alternative terms have included ‘gastroparesis-like syndrome’ and

'vomiting of unexplained etiology', while the Rome III system introduced 'chronic idiopathic nausea' and 'functional vomiting' within more restrictive scopes.

Methodological advances will be necessary to apply these findings to clinical diagnostics in future, in order to reduce the invasiveness of current gastric HR mapping methods. Significant technical hurdles must be overcome, including endoscopic device development, reliable methods of automated real-time data analysis, and cost reductions in acquisition equipment.[12,13] In addition, therapeutic trials will ultimately be required, to assess whether gastric dysrhythmias can be reversed in a way that meaningfully improves symptoms and quality of life in affected patients.

In conclusion, ICC and bioelectrical abnormalities were found in CUNV patients, similar to changes occurring in gastroparesis. These findings offer new pathogenic mechanisms underlying CUNV, and may inform future therapies.

Supplementary Material

Refer to Web version on PubMed Central for supplementary material.

Acknowledgments

We thank the clinical research and operating room staff at the University of Mississippi Medical Center, and Mr Simon Bull and Ms Rachel Berry for their valued assistance.

TLA is a licensor, consultant, and investigator for Medtronic, Inc.

Funding

This work was supported by the New Zealand Health Research Council, National Institutes of Health and the Gastroparesis Clinical Research Consortium (R01 DK64775, DK57061, DK73983, DK74008, and U01 DK074007). GOG thanks the American Neurogastroenterology and Motility Society (ANMS) for the Young Investigator Clinical Research Grant that enabled this collaboration. PD was supported by the Rutherford Foundation Trust, and Marsden Fund.

Abbreviations

CUNV	Chronic unexplained nausea and vomiting
GpCRC	Gastroparesis Clinical Research Consortium
ICC	Interstitial cells of Cajal
PCB	Printed circuit board
SD	Standard deviation
SEM	Standard error of the mean
HR	High-resolution

REFERENCES

1. Olden KW, Crowell MD. Chronic nausea and vomiting: new insights and approach to treatment. Curr. Treat Options Gastroenterol. 2005; 8:305–310. [PubMed: 16009031]

2. Pasricha PJ, Colvin R, Yates K, et al. Characteristics of patients with chronic unexplained nausea and vomiting and normal gastric emptying. Clin. Gastroenterol. Hepatol. 2011; 9:567–576. e1–e4. [PubMed: 21397732]

3. Anaparthy R, Pehlivanov N, Grady J, et al. Gastroparesis and gastroparesis-like syndrome: response to therapy and its predictors. Dig. Dis. Sci. 2009; 54:1003–1010. [PubMed: 19277867]

4. Gourcerol G, Leblanc I, Leroi AM, et al. Gastric electrical stimulation in medically refractory nausea and vomiting. Eur. J. Gastroenterol. Hepatol. 2007; 19:29–35. [PubMed: 17206074]

5. Hasler WL. Gastroparesis: pathogenesis, diagnosis and management. Nat. Rev. Gastroenterol. Hepatol. 2011; 8:438–453. [PubMed: 21769117]

6. Kashyap P, Farrugia G. Diabetic gastroparesis: what we have learned and had to unlearn in the past 5 years. Gut. 2010; 59:1716–1726. [PubMed: 20871131]

7. Grover M, Farrugia G, Lurken MS, et al. Cellular changes in diabetic and idiopathic gastroparesis. Gastroenterology. 2011; 140(5):1575-85.e8. [PubMed: 21300066]

8. Faussone-Pellegrini MS, Grover M, Pasricha PJ, et al. Ultrastructural differences between diabetic and idiopathic gastroparesis. J. Cell. Mol. Med. 2012; 16:1573–1581. [PubMed: 21914127]

9. O'Grady G, Angeli TR, Du P, et al. Abnormal initiation and conduction of slow-wave activity in gastroparesis, defined by high-resolution electrical mapping. Gastroenterology. 2012; 143:589–598. e1–e3. [PubMed: 22643349]

10. Abell TL, Familoni B, Voeller G, et al. Electrophysiologic, morphologic, and serologic features of chronic unexplained nausea and vomiting: lessons learned from 121 consecutive patients. Surgery. 2009; 145:476–485. [PubMed: 19375605]

11. Lin Z, Sarosiek I, Forster J, et al. Association of the status of interstitial cells of Cajal and electrogastrogram parameters, gastric emptying and symptoms in patients with gastroparesis. Neurogastroenterol. Motil. 2010; 22:56–61. e10. [PubMed: 19614868]

12. Cheng LK, Du P, O'Grady G. Mapping and modeling gastrointestinal bioelectricity: from engineering bench to bedside. Physiology (Bethesda). 2013; 28:310–317. [PubMed: 23997190]

13. O'Grady G, Wang T, Du P, et al. Recent progress in gastric arrhythmia: pathophysiology, clinical significance and future horizons. Clin. Exp. Pharmacol. Physiol. 2014; 41:854–862. [PubMed: 25115692]

14. Koch KL. Gastric dysrhythmias: a potential objective measure of nausea. Exp. Brain Res. 2014; 232:2553–2561. [PubMed: 24916149]

15. Abell TL, Adams KA, Boles RG, et al. Cyclic vomiting syndrome in adults. Neurogastroenterol. Motil. 2008; 20:269–284. [PubMed: 18371009]

16. Abell TL, Camilleri M, Donohoe K, et al. Consensus recommendations for gastric emptying scintigraphy: a joint report of the American Neurogastroenterology and Motility Society and the Society of Nuclear Medicine. Am. J. Gastroenterol. 2008; 103:753–763. [PubMed: 18028513]

17. Tougas G, Eaker EY, Abell TL, et al. Assessment of gastric emptying using a low fat meal: establishment of international control values. Am. J. Gastroenterol. 2000; 95:1456–1462. [PubMed: 10894578]

18. Hasler WL, Soudah HC, Dulai G, et al. Mediation of hyperglycemia-evoked gastric slowwave dysrhythmias by endogenous prostaglandins. Gastroenterology. 1995; 108:727–736. [PubMed: 7875475]

19. Gomez-Pinilla PJ, Gibbons SJ, Sarr MG, et al. Changes in interstitial cells of Cajal with age in the human stomach and colon. Neurogastroenterol. Motil. 2011; 23:36–44. [PubMed: 20723073]

20. Koch, KL.; Stern, RM. Handbook of electrogastrography. Oxford: Oxford University Press; 2004.

21. Grover M, Bernard CE, Pasricha PJ, et al. Clinical-histological associations in gastroparesis: results from the Gastroparesis Clinical Research Consortium. Neurogastroenterol. Motil. 2012; 24:531–539. e249. [PubMed: 22339929]

22. O'Grady G, Du P, Cheng LK, et al. Origin and propagation of human gastric slow-wave activity defined by high-resolution mapping. Am. J. Physiol. Gastrointest. Liver Physiol. 2010; 299:G585–G592. [PubMed: 20595620]

23. Angeli TR, Du P, Paskaranandavadivel N, et al. The bioelectrical basis and validity of gastrointestinal extracellular slow wave recordings. J. Physiol. 2013; 591:4567–4579. [PubMed: 23713030]

24. Du P, O'Grady G, Egbuji JU, et al. High-resolution mapping of in vivo gastrointestinal slow wave activity using flexible printed circuit board electrodes: methodology and validation. Ann. Biomed. Eng. 2009; 37:839–846. [PubMed: 19224368]
25. O'Grady, G.; Angeli, TR.; Lammers, WJEP. The principles and practice of gastrointestinal high-resolution electrical mapping. In: Cheng, LK.; Farrugia, G., editors. New Advances in Gastrointestinal Motility Research. Dordrecht: Springer Netherlands; 2013. p. 51-69.
26. Walldén J, Lindberg G, Sandin M, et al. Effects of fentanyl on gastric myoelectrical activity: a possible association with polymorphisms of the μ-opioid receptor gene? Acta anaesthesiol. Scand. 2008; 52:708–715. [PubMed: 18419726]
27. Yassi R, O'Grady G, Paskaranandavadivel N, et al. The gastrointestinal electrical mapping suite (GEMS): software for analyzing and visualizing high-resolution (multielectrode) recordings in spatiotemporal detail. BMC Gastroenterol. 2012; 12:60. [PubMed: 22672254]
28. Paskaranandavadivel N, O'Grady G, Du P, et al. Comparison of filtering methods for extracellular gastric slow wave recordings. Neurogastroenterol. Motil. 2013; 25:79–83. [PubMed: 22974243]
29. Erickson JC, O'Grady G, Du P, et al. Falling-edge, variable threshold (FEVT) method for the automated detection of gastric slow wave events in high-resolution serosal electrode recordings. Ann. Biomed. Eng. 2010; 38:1511–1529. [PubMed: 20024624]
30. Erickson JC, O'Grady G, Du P, et al. Automated gastric slow wave cycle partitioning and visualization for high-resolution activation time maps. Ann. Biomed. Eng. 2011; 39:469–483. [PubMed: 20927594]
31. Parkman HP, Hasler WL, Barnett JL, et al. Electrogastrography: a document prepared by the gastric section of the American Motility Society Clinical GI Motility Testing Task Force. Neurogastroenterol. Motil. 2003; 15:89–102. [PubMed: 12680908]
32. Paskaranandavadivel N, O'Grady G, Du P, et al. An improved method for the estimation and visualization of velocity fields from gastric high-resolution electrical mapping. IEEE. Trans. Biomed. Eng. 2012; 59:882–889. [PubMed: 22207635]
33. O'Grady G, Du P, Paskaranandavadivel N, et al. Rapid high-amplitude circumferential slow wave propagation during normal gastric pacemaking and dysrhythmias. Neurogastroenterol. Motil. 2012; 24:e299–e312. [PubMed: 22709238]
34. O'Grady G, Egbuji JU, Du P, et al. High-resolution spatial analysis of slow wave initiation and conduction in porcine gastric dysrhythmia. Neurogastroenterol. Motil. 2011; 23:e345–e355. [PubMed: 21714831]
35. Angeli TR, O'Grady G, Du P, et al. Circumferential and functional re-entry of in vivo slow-wave activity in the porcine small intestine. Neurogastroenterol. Motil. 2013; 25:e304–e314. [PubMed: 23489929]
36. Huizinga JD, Zarate N, Farrugia G. Physiology, injury, and recovery of interstitial cells of Cajal: basic and clinical science. Gastroenterology. 2009; 137:1548–1556. [PubMed: 19778538]
37. Lammers WJ, Ver Donck L, Stephen B, Smets D, Schuurkes JA. Focal activities and re-entrant propagations as mechanisms of gastric tachyarrhythmias. Gastroenterology. 2008; 135:1601–1611. [PubMed: 18713627]
38. Lammers WJEP, Stephen B, Karam SM. Functional reentry and circus movement arrhythmias in the small intestine of normal and diabetic rats. Am. J. Physiol. Gastrointest. Liver Physiol. 2012; 302:G684–G689. [PubMed: 22207580]
39. Lammers WJEP. Arrhythmias in the gut. Neurogastroenterol. Motil. 2013; 25:353–357. [PubMed: 23490042]
40. O'Grady G, Du P, Lammers WJEP, et al. High-resolution entrainment mapping of gastric pacing: a new analytical tool. Am. J. Physiol. Gastrointest. Liver Physiol. 2010; 298:G314–G321. [PubMed: 19926815]
41. Ladabaum U, Koshy SS, Woods ML, et al. Differential symptomatic and electrogastrographic effects of distal and proximal human gastric distension. Am. J. Physiol. 1998; 275:G418–G424. [PubMed: 9724252]
42. Kligfield P, Gettes LS, Bailey JJ, et al. Recommendations for the standardization and interpretation of the electrocardiogram, part I: the electrocardiogram and its technology. J. Am. Coll. Cardiol. 2007; 49:1109–1127. [PubMed: 17349896]

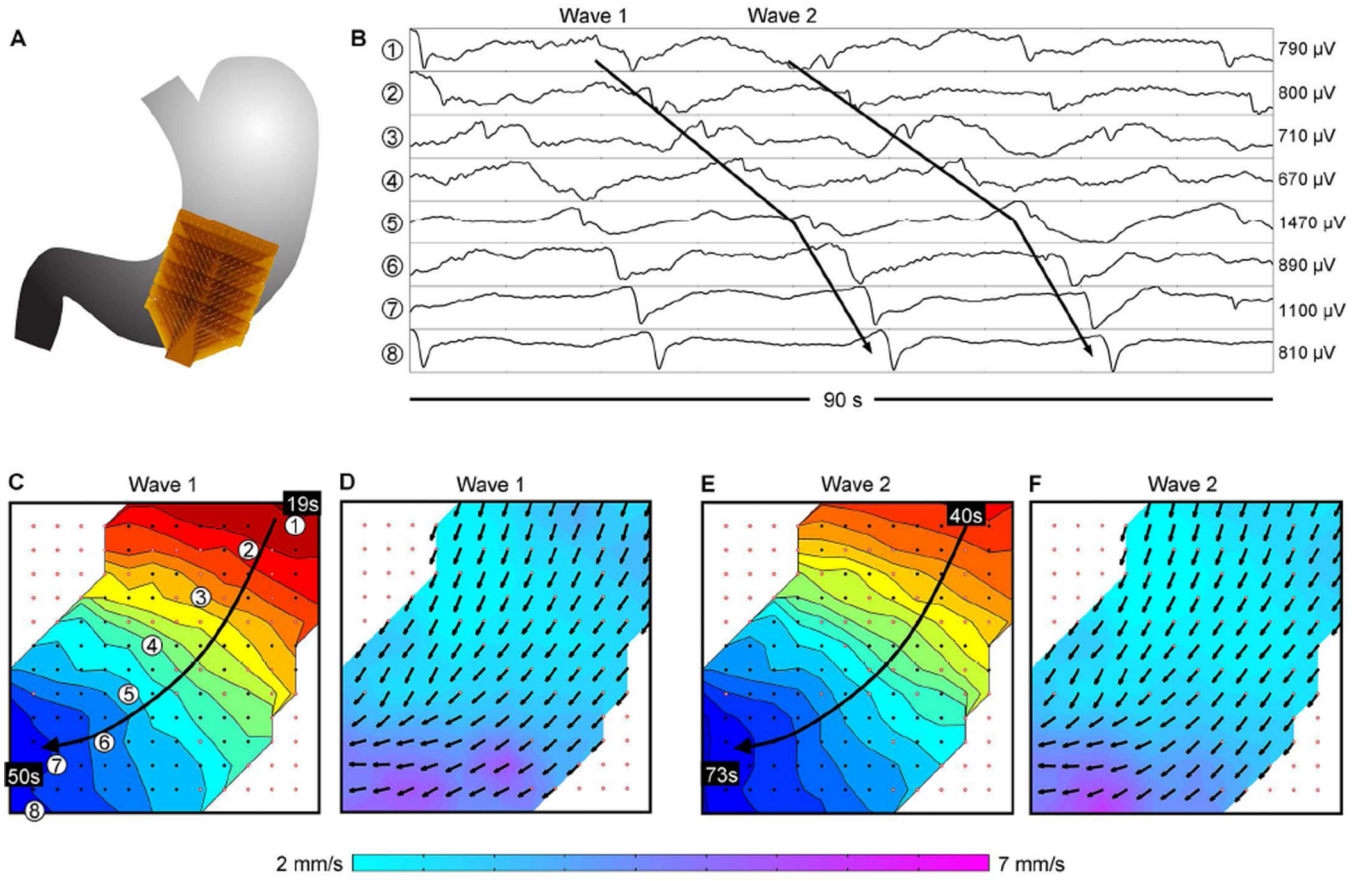

Figure 1.

Normal gastric slow wave propagation in a control. (**A**) Position of the array. (**B**) Electrograms from positions indicated in *C* (frequency, 2.8 ± 0.1 SD cycles/min). (**C**) Isochronal activation map of 'Wave 1' indicated in *B*, demonstrating normal antegrade propagation. Black dots represent electrodes, with white dots outlined red representing electrodes where activity was interpolated. Each color band shows the area of slow wave propagation per 2 seconds. (**D**) Velocity map of Wave 1, showing the speed (color spectrum) and direction (arrows) of the wavefront at each electrode. (**E,F**) Isochronal activation and velocity field maps of 'Wave 2' in *B*, demonstrating consistency of the antegrade propagation. See Supplementary Video 1 for animation.

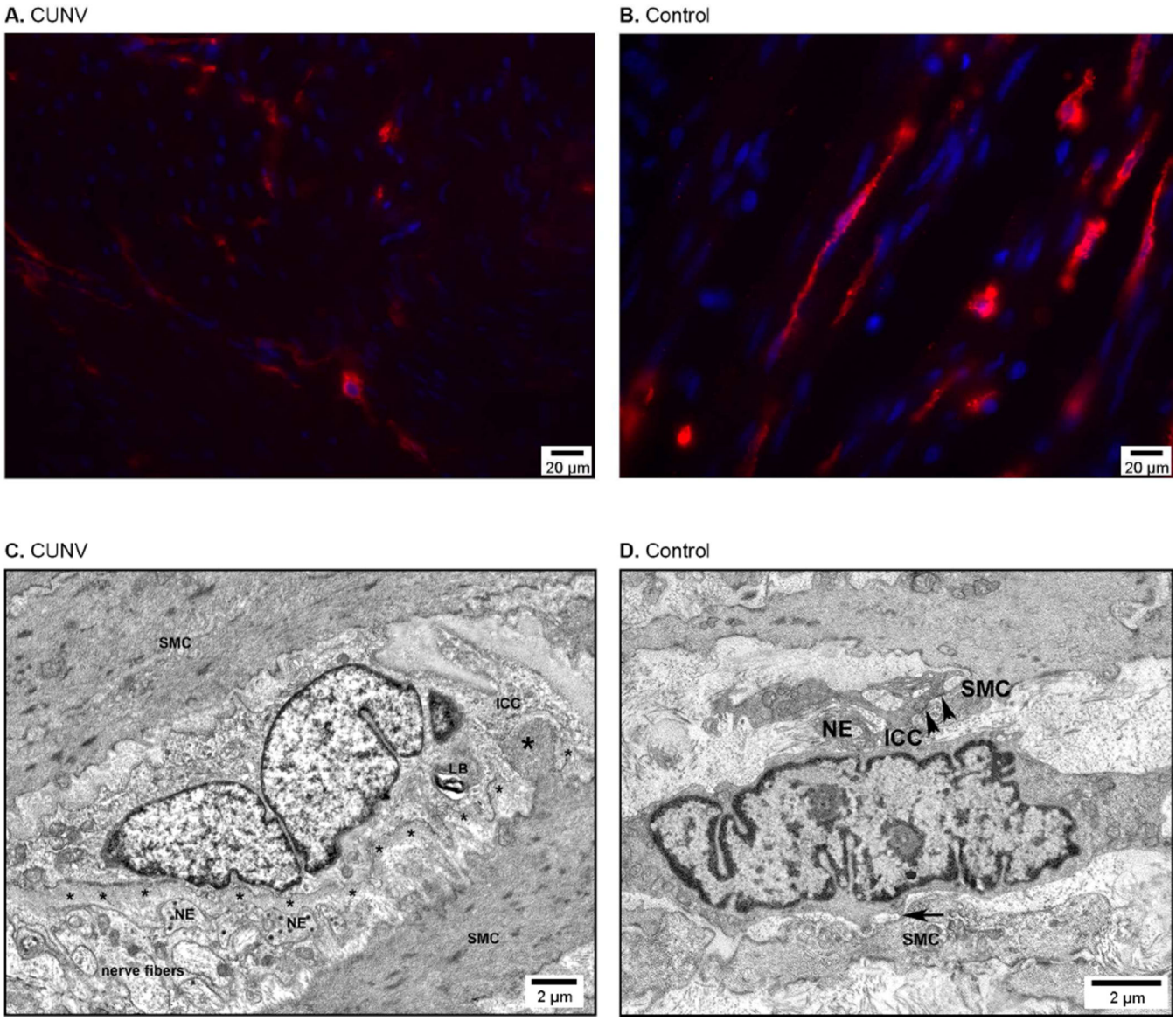

Figure 2.

(**A,B**) Representative images showing depletion of the ICC network in the gastric smooth muscle in a CUNV patient (*A*) compared to control (*B*). The red signal is Kit immunoreactivity marking ICC; the blue signal is 4',6'-diamidino-2-phenylindone counterstain marking cellular nuclei. (**C,D**) Electron microscopy images showing mild ultrastructural abnormalities in a CUNV patient (*C*) compared to control (*D*). Labeled structural components: thick basal lamina (small astericks), nerve endings (NE), smooth muscle cells (SMC), lamellar body (LB), ICC-SMC contact (arrows), and peg-and-socket junction (large astericks).

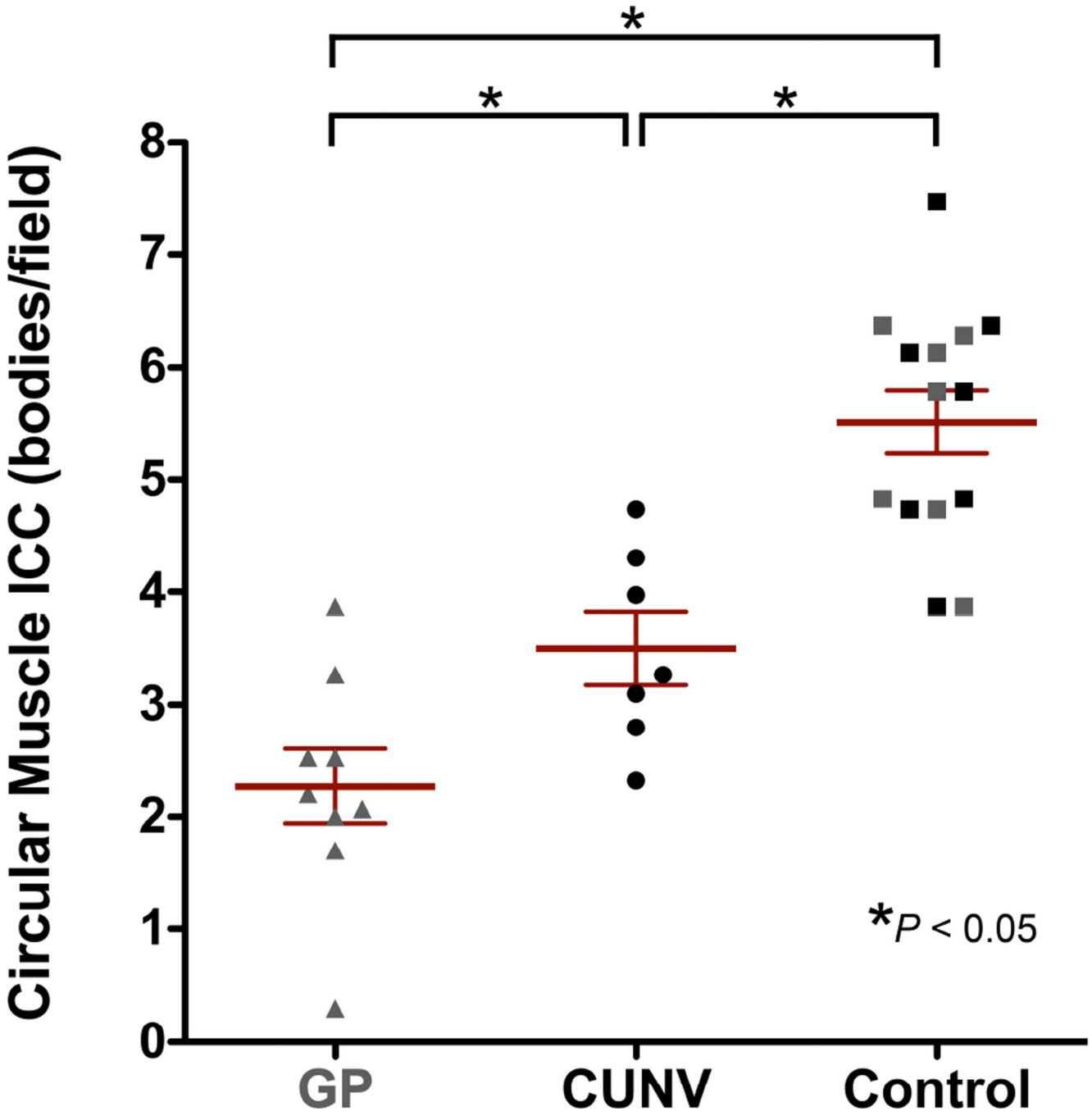

Figure 3.

Comparison of ICC density between CUNV patients and healthy controls. Data from a recent gastroparesis (GP) cohort[9] (in grey) are also displayed for comparison.

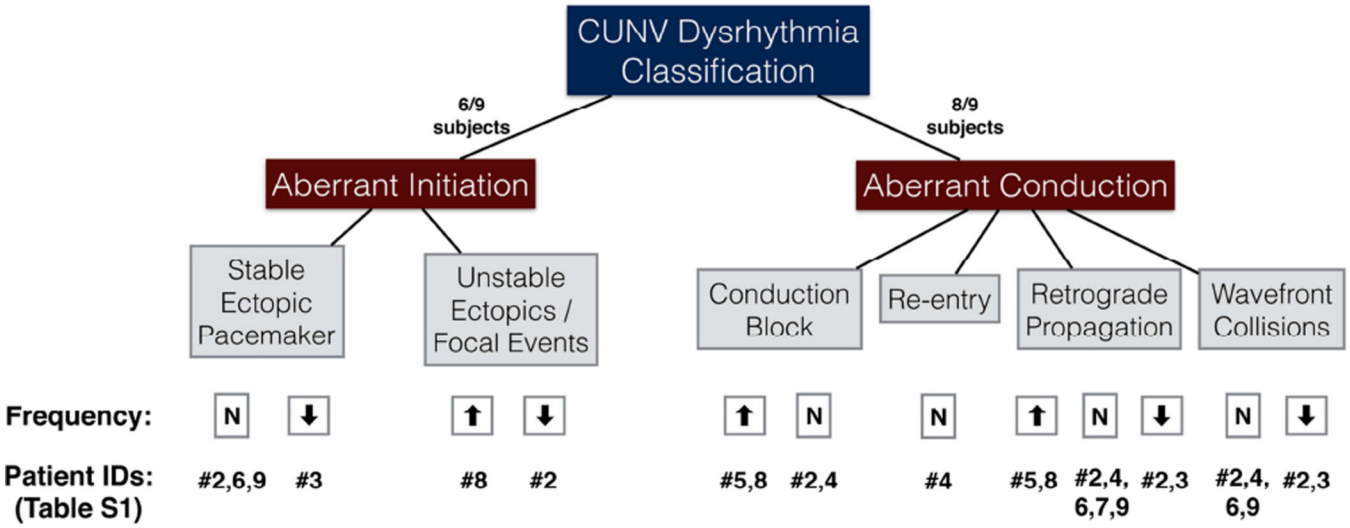

Figure 4.

Classification and occurrence of slow wave dysrhythmias mapped in CUNV patients. 'N' signifies normal frequency. There was one additional case (ID #5) of tachygastria of indeterminate origin, and a further case (ID #1) of apparent slow wave quiescence (see text).

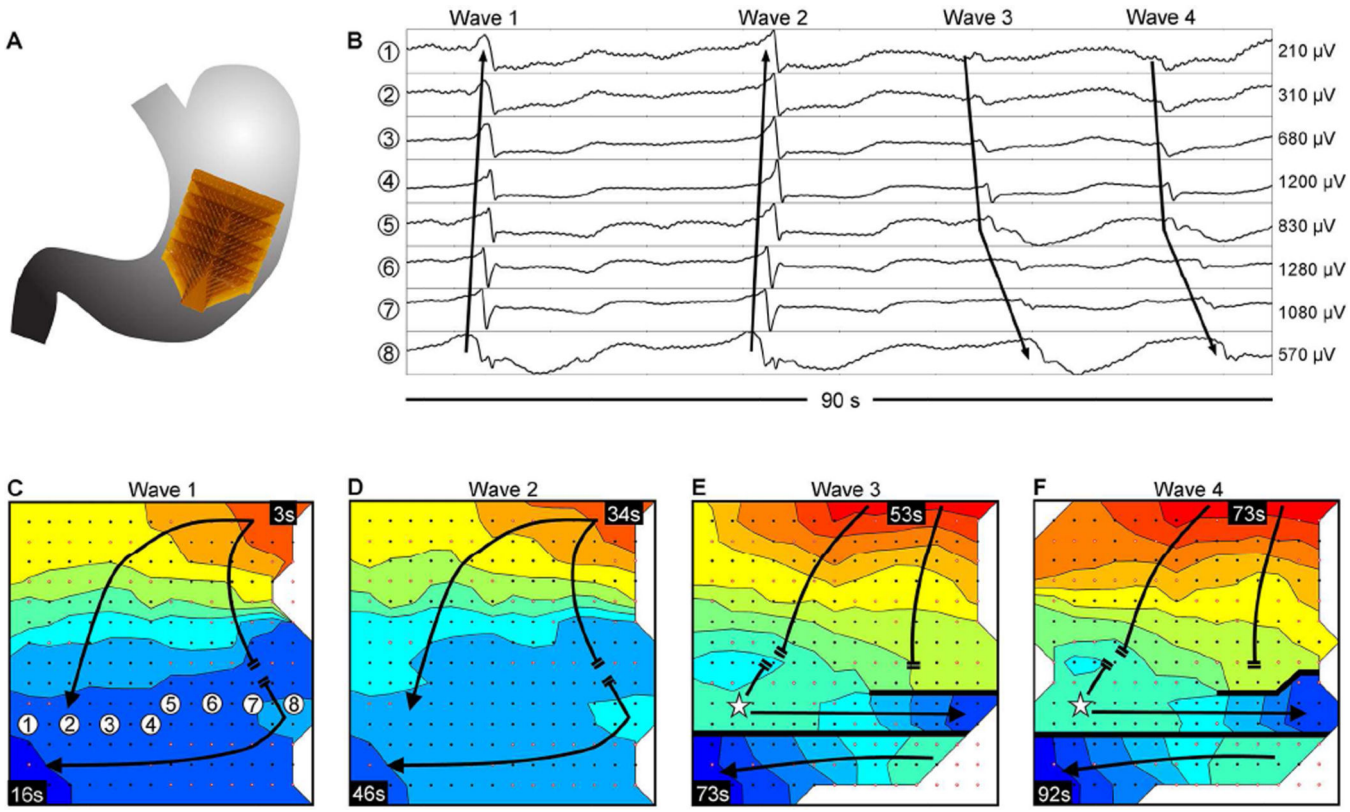

Figure 5.

Abnormal slow wave initiation and conduction; isochronal intervals = 1.5 seconds. (**A**) Position of the array. (**B**) Representative electrograms from positions indicated in *C*; propagation sequences are labeled based on their corresponding waves 1–4, shown in panels *C–F*. (**C**) Isochronal activation map. Slow wave activity propagated onto the array from the greater-curvature, colliding with an unstable focal activity on the distal portion of the array. (**D**) The unstable focal activity was consistent over a second cycle. (**E**) A new stable ectopic pacemaker emerged in the distal portion of the array (represented by a *star*), initiating retrograde propagation that collided with the uncoupled antegrade wavefront. Circumferential propagation was out-of-phase with distal activity that was propagating in the opposite direction circumferentially, resulting in a complete functional conduction block (thick black line). (**F**) Propagation repeated as described in *E*, with stability of the ectopic pacemaker and distal block that remained consistent through the end of the recording period. A frequency increase occurred between the unstable focal activity of *C&D* (bradygastric, 2.0 ± 0.1 cycles/min) and the stable ectopic activity of *E&F* (normal frequency, 3.2 ± 0.2 cycles/min). See Supplementary Video 2 for animation.

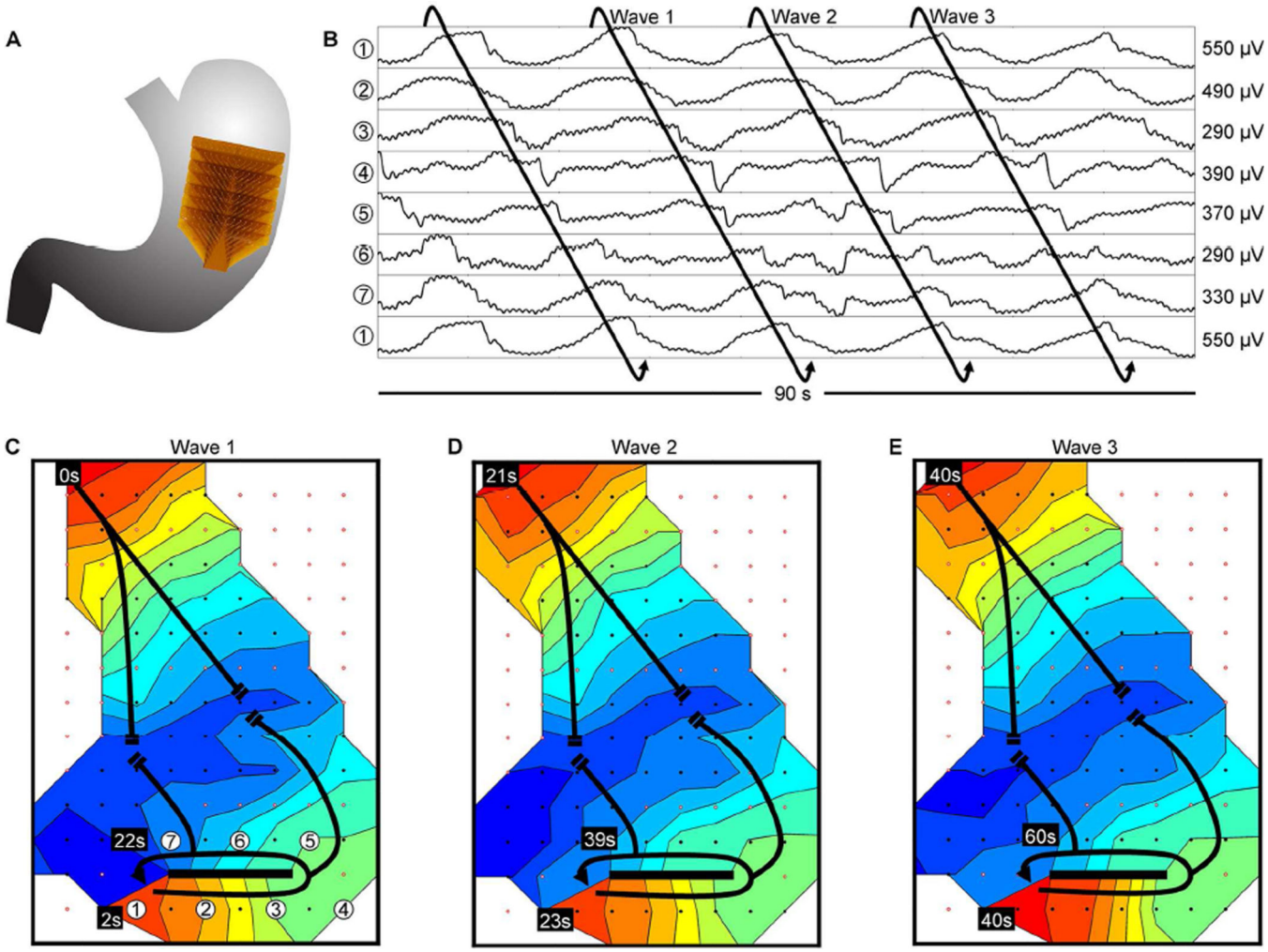

Figure 6.

Slow wave re-entry; isochronal intervals = 2 seconds. (**A**) Position of the array. (**B**) Representative electrograms from positions indicated in *C*; electrode 1 is repeated at the bottom of the electrograms to illustrate the continuity of the re-entrant circuit. (**C–E**) Isochronal activation maps. Activation propagated in a circuit around a linear conduction block (thick black line), re-activating that same circuit over successive cycles, thereby establishing re-entry (frequency, 3.3 ± 0.2 cycles/min). Slow wave activity propagated outward from the re-entrant circuit, in part colliding with an uncoupled antegrade-propagating wavefront. See Supplementary Video 3 for animation.

Table 1

Comparison of characteristics between the CUNV population and mapping controls. Methods of mapping and data analysis were identical.

Characteristic	CUNV cohort	Control cohort
No. of patients	9	9
Median age, y (range)	50 (22–59)*	57 (25–74)*
Sex (female:male)	8:1	5:4
No. of recordings	18	11
Duration of mapping (mean ± SD)	11 ± 5 min/pt	10 ± 3 min/pt
Anesthetic regimen	Prophylactic antibiotics, benzodiazepine premedication, a short-acting intravenous opiate, muscle relaxants (suxamethonium or rocuronium), propofol, desflurane	Prophylactic antibiotics, benzodiazepine premedication, a short-acting intravenous opiate, muscle relaxant (atracurium or suxamethonium), propofol, isoflurane, or sevoflurane. Eight also had epidural or spinal block.
Electrodes (type; tip diameter; no. of channels)	PCB[24]; 0.3 mm; 256 channels	PCB[24]; 0.3 mm; 96–256 channels
Filtering methods	Savitzky-Golay (1.7s window; polynomial order 9) and moving median (20s window) filters[28]	
Analysis and isochronal activation mapping methods	FEVT, REGROUPS, and SIV algorithms performed in GEMS v1.5 with subsequent manual review[27,29,30]	
Frequency, velocity, and amplitude calculation methods	Algorithms in GEMS v1.5[27]	

* $P = 0.14$.